Table S1. List of drugs taken by ICB-treated melanoma patients, related to Figure 1.

Drug name	Alive NO.	Deceased NO.	Deceased %	Fisher exact test
Acetaminophen (Tylenol)	81	75	0.48	0.03
Antiarthritics	225	138	0.38	0.90
Antiasthmatics	79	61	0.44	0.26
Antibiotics	185	143	0.44	0.13
Anticoagulants	63	77	0.55	0.00
Antiemetic -phenothiazines	90	111	0.55	0.00
Antihistamines-1st	163	116	0.42	0.40
Antihistamines-2nd	95	38	0.29	0.03
Antiplatelet drugs	130	65	0.33	0.19
Aspirin	166	65	0.28	0.00
Atorvastatin	70	53	0.43	0.38
Azithromycin	22	10	0.31	0.46
Cephalosporin (1st-4th generations)	35	23	0.40	0.89
Codeine	41	18	0.31	0.27
Dabrafenib mesylate	41	44	0.52	0.02
Diphenhydramine HCL	88	72	0.45	0.14
Docusate sodium	57	45	0.44	0.29
Esomeprazole (Meganesium)	27	15	0.36	0.75
Fluoroquinolones	46	36	0.44	0.35
Glucocorticoid	131	107	0.45	0.09
Hydrochlorothiazide	36	17	0.32	0.38
Hydrocortisone	57	39	0.41	0.74
Lbuprofen	108	60	0.36	0.49
Levothyroxine	177	113	0.39	0.94
Loratadine	117	87	0.43	0.30
Metformin	70	51	0.42	0.49
Metoprolol tartrate	40	31	0.44	0.45
Morphine (morphine sulfate)	17	52	0.75	0.00
Omeprazole	45	49	0.52	0.01
Ondansetron	140	166	0.54	0.00
Oxycodone	56	68	0.55	0.00
Penicillin	43	34	0.44	0.39
Prednisone	60	50	0.45	0.18
Ranitidine hydrochloride	23	12	0.34	0.72
Salicylate anglgesics	133	65	0.33	0.14
Simvastatin	43	30	0.41	0.71
Tatracycline antibiotics	34	26	0.43	0.50
Tramadol	158	135	0.46	0.03
Trametinib	29	45	0.61	0.00
Valsartan	21	6	0.22	0.11

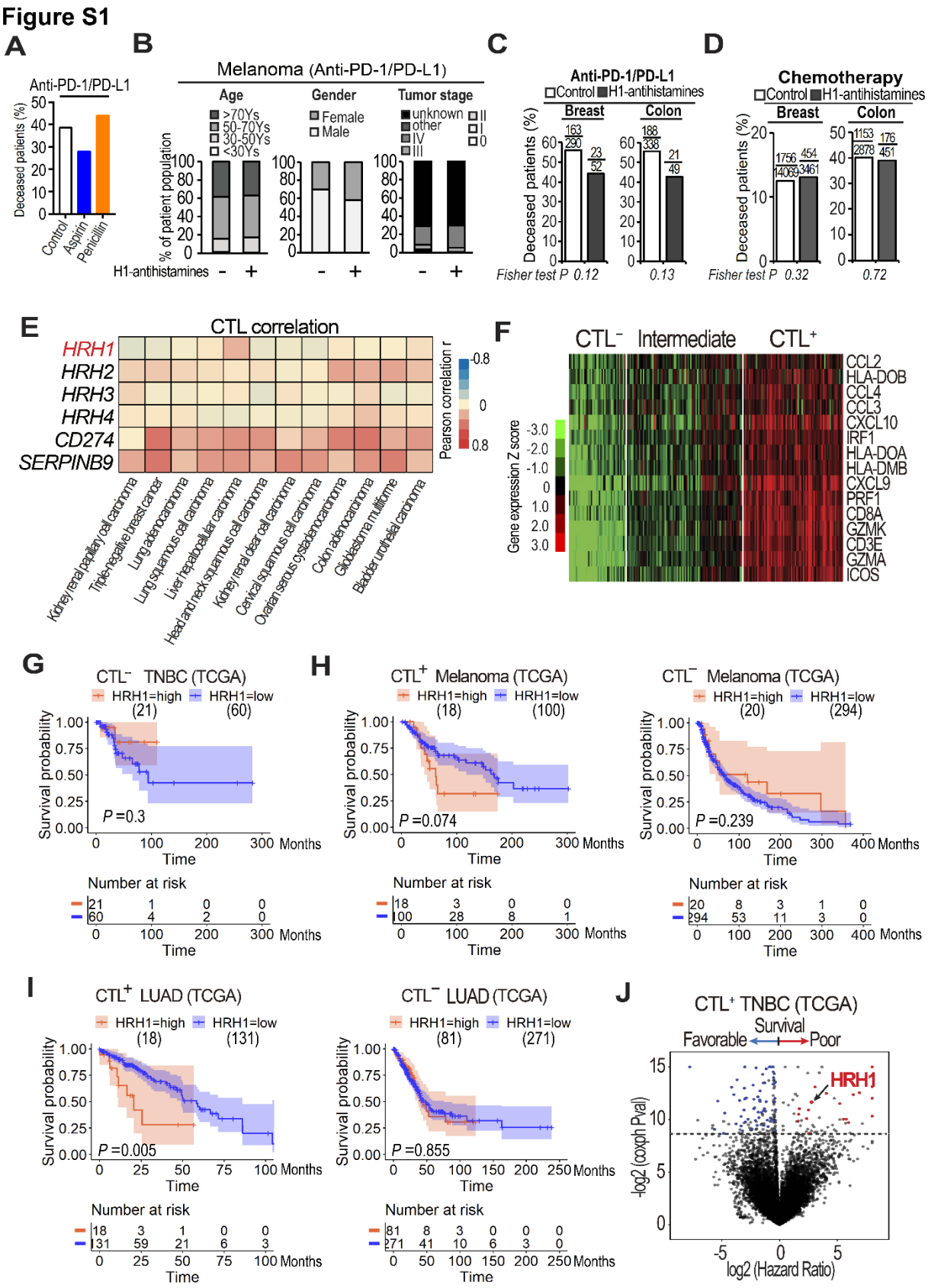

Figure S1. Correlations between *HRH1* expression and patients' clinical outcomes in CTL$^+$ tumors across multiple cancer types, related to Figure 1.

(**A**) Percentages of deceased cancer patients taking aspirin or penicillin during anti-PD-1/PD-L1 treatment *versus* those did not. (**B**) The distributions of age-, sex-, and tumor stages among melanoma patients encountered at MD Anderson who took H1-antihistamines during immunotherapy compared with those who did not. (**C**) Percentages of deceased cancer patients taking H1-antihistamines during anti-PD-1/PD-L1 treatment *versus* those did not (Fisher exact test). (**D**)

Percentages of deceased cancer patients taking H1-antihistamines during chemotherapy treatment *versus* those did not (Fisher exact test). (**E**) Pearson correlations between histamine receptors (*HRH1-4*) and CTL in the indicated cancer types analyzed by TIDE. *CD274* (*PD-L1*) and *SERPINB9* were used as controls. Color gradient represents low to high Person correlation coefficient. (**F**) Heatmap of gene expression values depicting CTL-related 15-gene signature in CTL^- (n=42), intermediate (n=86), and CTL^+ groups (n=74). Color gradient represents low (green) to high (red) normalized Z scores of each gene across samples. (**G-I**) Kaplan-Meier survival analysis of low *HRH1* (blue) versus high *HRH1* (red) expression in CTL^- TNBC (**F**), in CTL^+ or CTL^- melanoma (**G**), and in CTL^+ or CTL^- lung adenocarcinoma (LUAD) (**H**) in TCGA datasets. The numbers at risk are the stratified *HRH1* level high and low patient numbers of those who remained alive and uncensored after a certain time period. (**J**) Volcano plots of hazard ratios and −log2 (*P* values) from the coxph analysis of CTL^+ triple-negative breast cancer (TNBC) in TCGA dataset. Black, all 16,975 genes. Red and blue, genes associated with poor and favorable outcomes, respectively. Horizontal dashed line marks a threshold *P* value of 0.0025.

Table S2. Information of antihistamines uptake in cancer patients, related to Figure1.

Patient cancer type	Category		Patient No.	Antihistamines uptake**		
				YES	NO	*P*-value
Melanoma patients (2016-2017)	Gender	Male	598	58	540	0.031
		Female	280	41	239	
		Sum	878	99	779	
	Age (years)	<50	131	14	117	0.896
		50-70	380	45	335	
		>70	367	40	327	
		Sum	878	99	779	
	Stage*	0-I	23	2	21	0.153
		II	15	0	15	
		III	83	14	69	
		IV	298	41	257	
		Others &	502	51	451	
Breast Cancer Patients (2016-2018)	Gender	Male		NA	NA	
		Female	342	52	290	
	Age (years)	<50	68	10	58	0.992
		50-70	157	24	133	
		>70	117	18	99	
		Sum	342	52	290	
	Stage*	0-I	27	6	21	0.3315
		II	44	6	38	
		III	57	5	52	
		IV	90	16	74	
		Others &	173	28	145	

(Continued) Table S2. Information of antihistamines uptake in cancer patients, related to Figure 1.

Patient cancer type	Category		Patient No.	Antihistamines uptake**		
				YES	NO	*P*-value
Lung Cancer Patients (2016-2018)	Gender	Male	1137	135	1002	0.562
		Female	800	102	698	
		Sum	1937	237	1700	
	Age (Years)	<50	130	12	118	0.400
		50-70	969	115	854	
		>70	838	110	728	
		Sum	1937	237	1700	
	Stage*	0-I	79	11	68	0.698
		II	56	7	49	
		III	113	12	101	
		IV	466	69	397	
		Others &	1284	149	1135	
Colon Cancer Patients (2016-2018)	Gender	Male	205	26	179	0.989
		Female	182	23	159	
		Sum	387	49	338	
	Age (years)	<50	79	10	69	0.857
		50-70	194	23	171	
		>70	114	16	98	
		Sum	387	49	338	
	Stage*	0-I	4	1	3	0.898
		II	6	1	5	
		III	17	2	15	
		IV	120	22	98	
		Others &	253	26	227	

*Some patients were diagnosed with different stages of cancer at different time points and may have been counted more than once.

** Patients took 2nd generation antihistamines during ICB-treatment and had no allergy status reported within 10 days before the treatment.

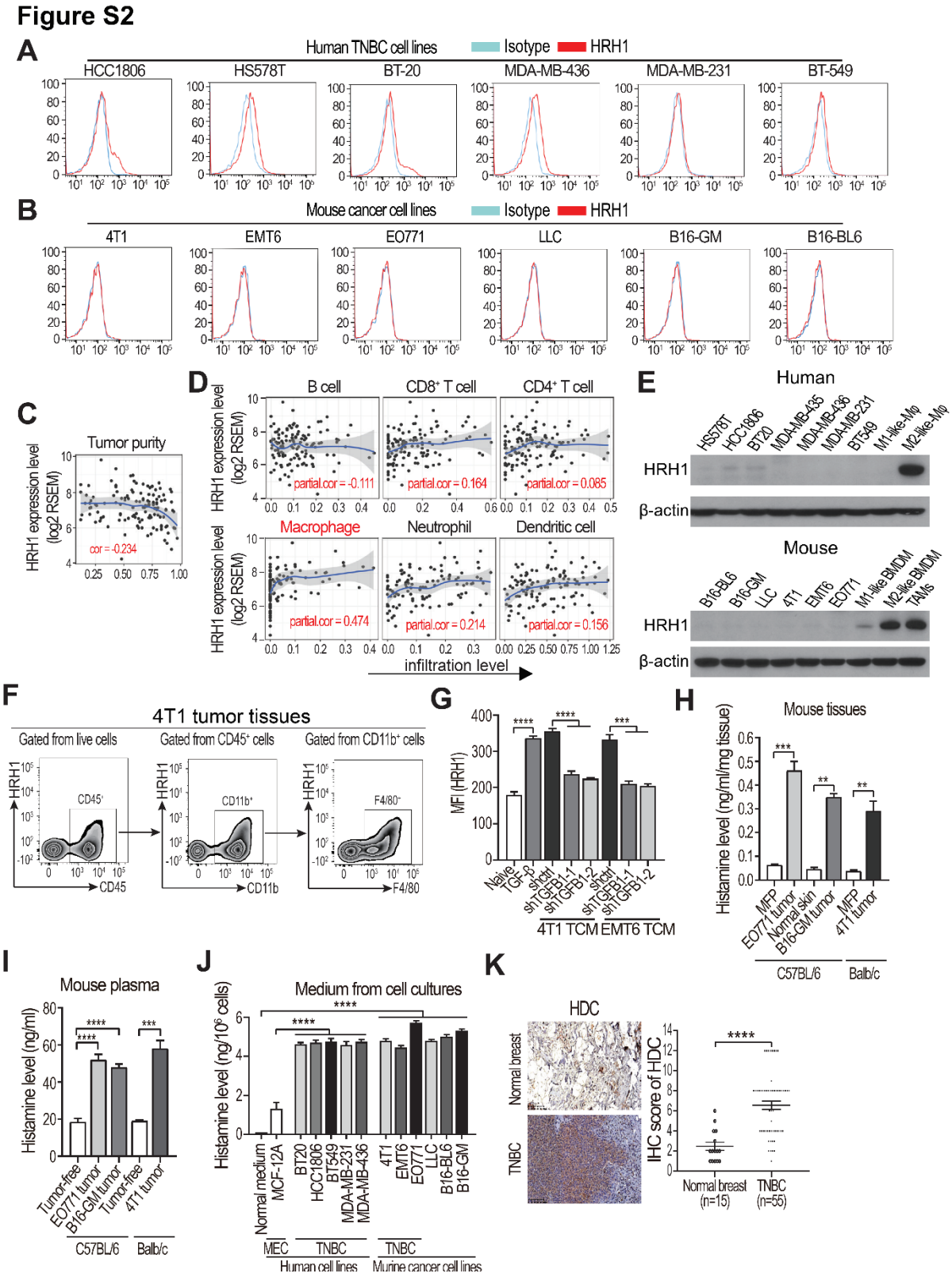

Figure S2. HRH1 expression in cancer cell lines and macrophages, related to Figure 2.

(**A** and **B**) Flow cytometry analysis of HRH1 expression on human (A) and mouse (B) cancer cell lines. Blue, Isotype control; Red, HRH1. (**C** and **D**) Analysis of correlations between *HRH1* expression and tumor purity (**C**), B-cells, $CD8^+$ T cells, $CD4^+$ T cells, macrophages, and neutrophils (**D**) in TCGA basal-like breast cancers using Tumor IMmune Estimation Resource (TIMER). The purity-corrected partial Spearman's correlation coefficient and statistical *P* value were presented. (**E**) Representative western blot analysis of HRH1 expression in human and mouse cancer cell lines, and macrophages. (**F**) Gating strategy to identify $HRH1^+$ subsets in 4T1 tumor. Single cells isolated from digested tumor tissues were gated for viable, hemopoietic cells ($CD45^+$), myeloids ($CD45^+CD11b^+$), and macrophages ($CD11b^+Gr1^-F4/80^+$). (**G**) MFI of HRH1 on naïve, TGF-β (20 ng/ml)-treated, or indicated TCM-treated BMDMs. TCM

was collected from scramble ctrl (shctrl) or TGF-β1 knocked down (shTGFB1) 4T1 or EMT6 cells (one-way ANOVA). (**H-J**) Histamine levels in culture medium from the indicated tumor tissues (**H**), blood plasma (**I**), and cell lines (**J**) were detected by ELISA. MEC, mammary epithelial cells (n=3-6, t-test or one-way ANOVA).(K) HDC expression in normal human breast tissues and TNBC tissues was detected by IHC. Mean ± SEM, ***P*<0.01, ****P*<0.001, *****P*<0.0001.

Figure S3

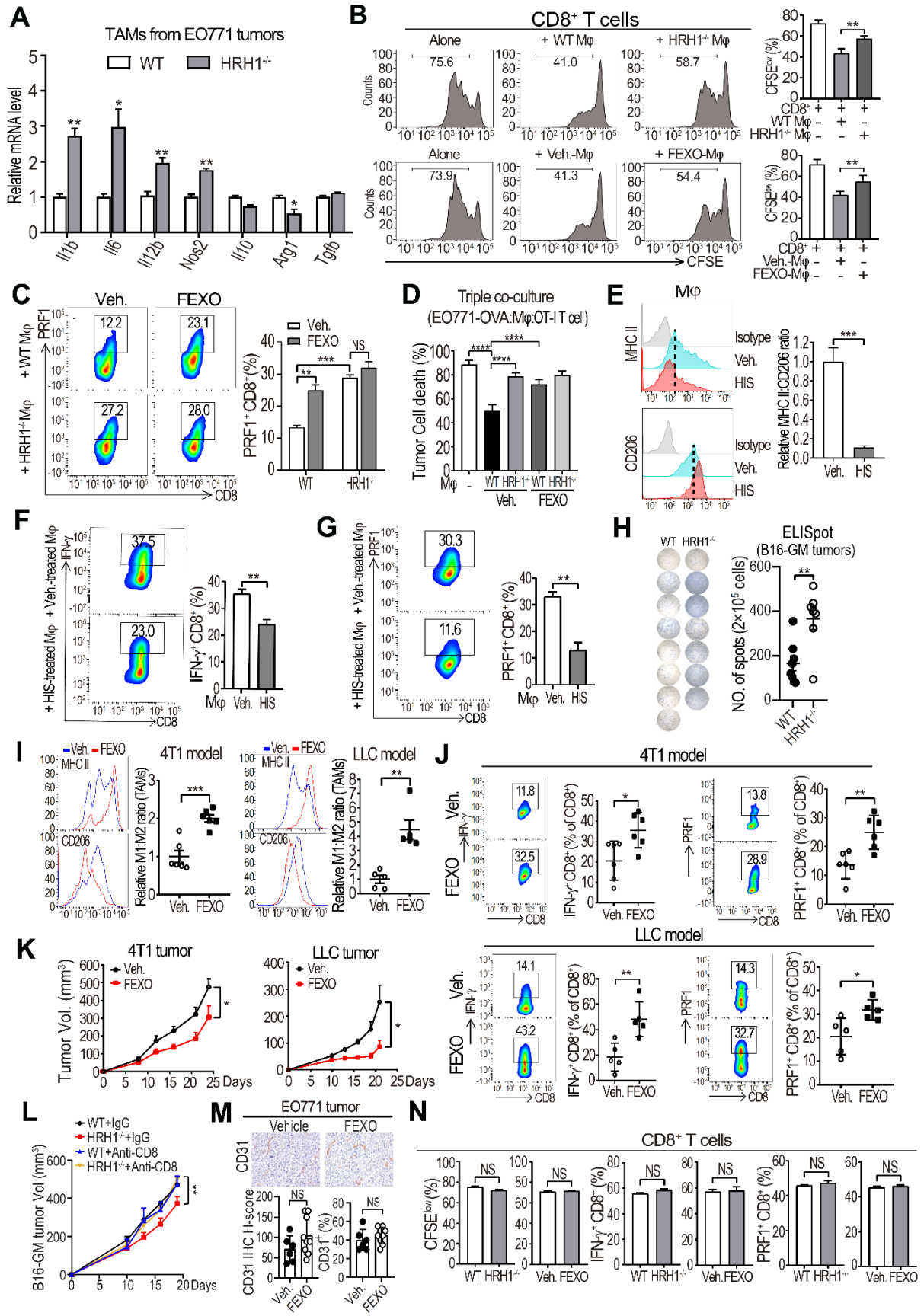

Figure S3. HRH1 inhibition enhances T cell anti-tumor activity, related to Figure 3.

(A) Relative mRNA levels of indicated M1 and M2 markers in TAMs of EO771 tumors growing in WT and HRH1$^{-/-}$ mice. (**B**) Representative histograms and evaluation of CD8^{+} T cell proliferation based on carboxyfluorescein succinimidyl ester (CFSE) dilution *in vitro*. CD3/CD28 activated T cells were co-cultured with WT, HRH1$^{-/-}$, vehicle- or FEXO (10 μM)-treated BMDMs (TCM-treated) for 24 hours before flow cytometry analysis. (**C**) Representative

flow cytometry analysis and quantification of splenic PRF1$^+$ CD8$^+$ T cells activated by CD3/CD28 *in vitro*. Activated T cells were first co-cultured with WT, HRH1$^{-/-}$, vehicle- or FEXO (10 μM)-treated BMDMs (TCM-treated) for 24 hours before flow cytometry analysis. (**D**) Estimation of OT1-mediated killing of EO771-OVA cells in the presence of WT BMDM, HRH1$^{-/-}$ BMDM, vehicle-treated or FEXO-treated BMDM (n=6, t-test). (**E**) Representative flow cytometry analysis and quantification of M1-like macrophage marker (MHCII$^+$) and M2-like macrophage marker (CD206$^+$) expression in vehicle- or histamine (HIS, 10 μM)-treated peritoneal macrophages. (**F** and **G**) Representative flow cytometry analysis and quantification of splenic IFN-γ$^+$ CD8$^+$ T cells (**F**) and PRF1$^+$ CD8$^+$ T cells (**G**) activated by CD3/CD28 *in vitro*. Activated T cells were first co-cultured with vehicle- or HIS (10 μM)-treated peritoneal macrophages for 24 hours before flow cytometry analysis. (**H**) Quantitation of tumor-reactive T cell frequency in B16-GM tumors by IFN-γ ELISPOT assay. (**I**) Relative MHC II:CD206 MFI ratio of tumor-associated macrophages (TAMs) in 4T1 and LLC tumors from vehicle-treated versus FEXO-treated WT mice (n=5-6, t-test). (**J** and **K**) Percentages of IFN-γ$^+$ or PRF1$^+$ CD8$^+$ T cells (**J**), and tumor growth (**K**) in 4T1 and LLC tumors from vehicle- or FEXO-treated mice (n=5-6, t-test for flow cytometry analysis; n= 6 mice per group, two-way ANOVA for tumor growth analysis). (**L**) B16-GM tumor growth with indicated treatment. CD8$^+$ T cells were depleted by anti-CD8 antibodies (n=6-7 mice/group, two-way ANOVA). (**M**) Evaluation of tumor blood vessel density by IHC staining of CD31 in EO771 tumors treated with vehicle or FEXO. Top: representative IHC staining slides; bottom: quantification of CD31 IHC staining using H-score (left) or CD31$^+$ cell percentage (right). (**N**) Comparison of CD8$^+$ T cell proliferation (CFSE dilution) and cytotoxic/cytolytic activities (IFN-γ$^+$ and PRF1$^+$) between WT *versus* HRH1$^{-/-}$, and vehicle- *versus* FEXO (10 μM)-treated CD8$^+$ T cells analyzed by flow cytometry (n=5, t-test). Mean ± SEM, **P*<0.05, ***P*<0.01, ****P*<0.001, *****P*<0.0001, NS: not significant.

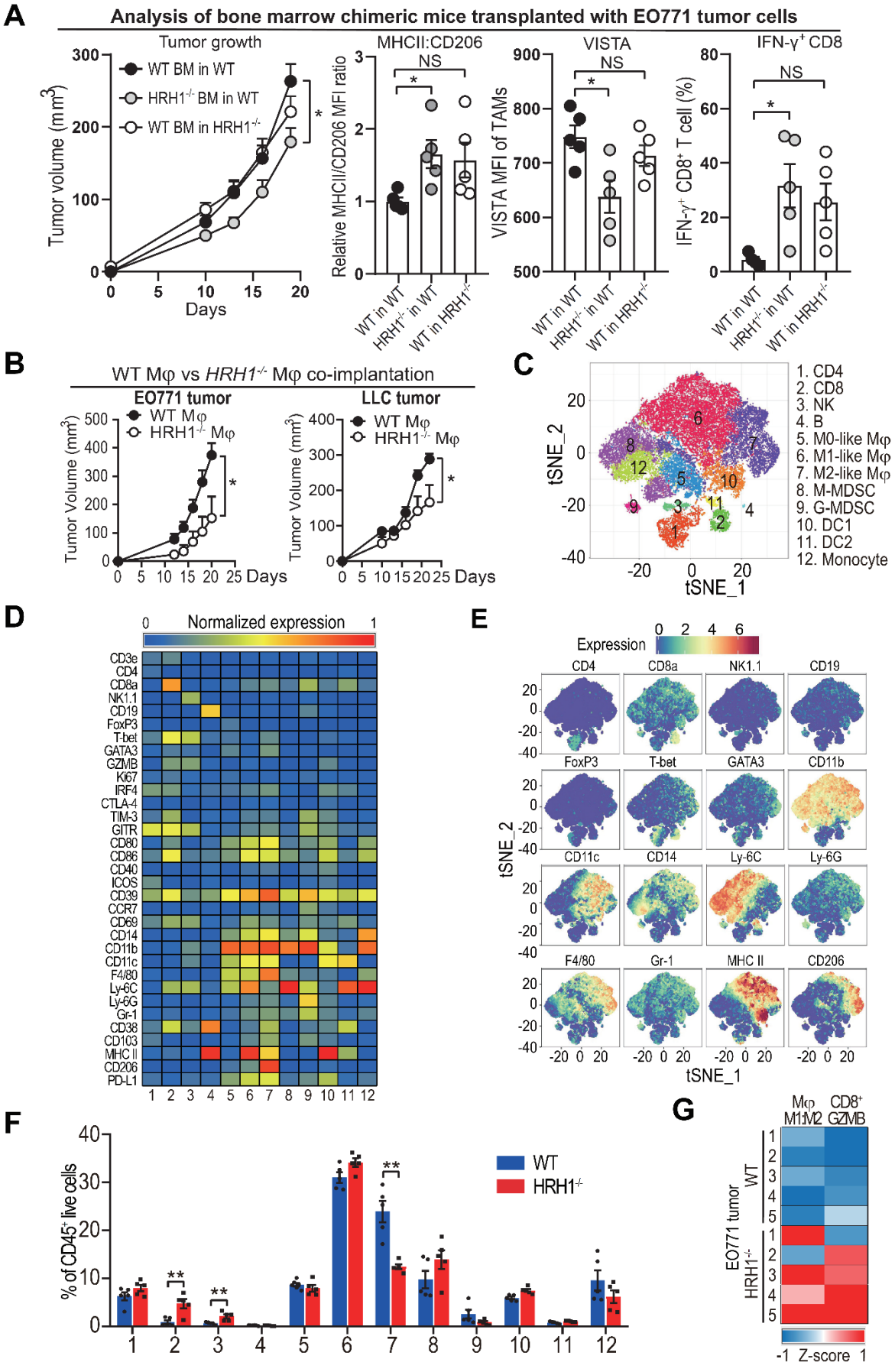

Figure S4. Bone marrow chimeric mice experiments, macrophage co-implantation and profiling of immune microenvironment of EO771 tumors by CyTOF, related to Figure 3.

(**A**)Tumor growth, MHCII:CD206 MFI ratio and VISTA expression in TAMs, and IFNγ^{+} CD8^{+} T cell infiltration in EO771 tumors from indicated chimeric mice. WT in WT: WT mice reconstituted with WT bone marrow cells; HRH1^{-}

$^{-/-}$ in WT: WT mice reconstituted with HRH1$^{-/-}$ bone marrows; WT in HRH1$^{-/-}$: HRH1$^{-/-}$mice reconstituted with WT bone marrows (n=6 mice/group, one-way ANOVA). (**B**) Growth of EO771 and LLC tumor cells co-implanted with WT or HRH1$^{-/-}$ BMDMs in WT recipient mice, respectively (n=6 mice/group, two-tailed t-test). (**C**) t-distributed stochastic neighbor embedding (tSNE) plot of TILs overlaid with color-coded clusters in EO771 tumors. (**D**) Heat map displaying normalized marker expression of each immune cluster. (**E**) tSNE plot of TILs overlaid with the expression of indicated markers. (**F**) Frequency of clusters of indicated immune cell subsets in EO771 tumors from WT and HRH1$^{-/-}$ mice (t-test). (**G**) M1:M2 ratios of macrophages (clusters 5, 6, and 7) and granzyme B (GZMB) expression in CD8 cluster (cluster 2) of each sample from WT and HRH1$^{-/-}$ mice (n=5/group). Mean ± SEM, **P*<0.05,***P*<0.01.

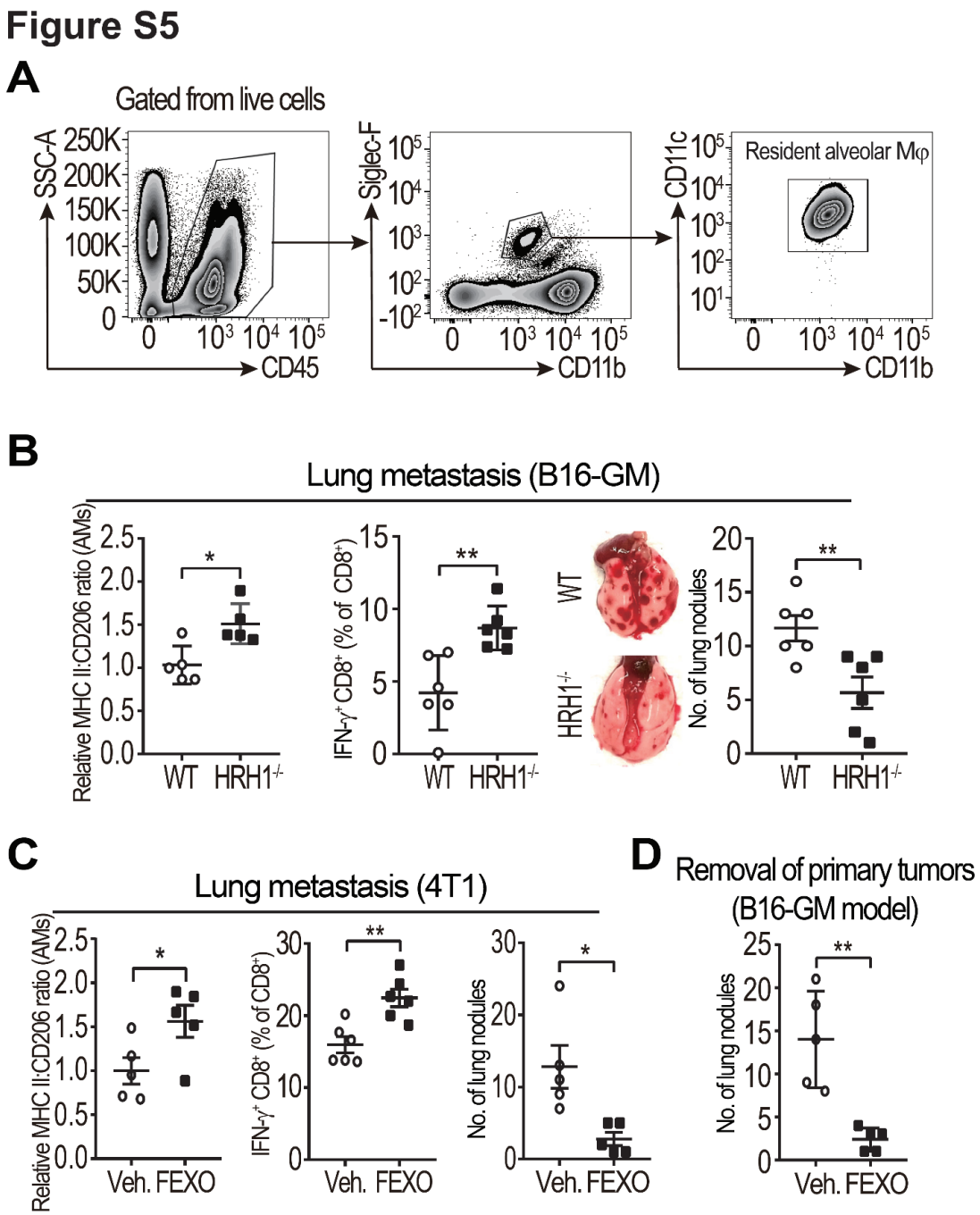

Figure S5. HRH1 inhibition enhances T cell anti-tumor activity in lung and inhibits lung metastasis, related to Figure 3.

(**A**) Gating strategy used to identify resident alveolar macrophage (AM) subset ($CD11b^{-}Siglec\text{-}F^{+}CD11C^{+}$) in mouse lung tissues. (**B** and **C**) Relative MHC II:CD206 MFI ratio of AMs, the percentage of IFN-γ^{+} $CD8^{+}$ T cells and lung metastatic nodules in lung tissues from B16-GM tumor-bearing WT *versus* $HRH1^{-/-}$ mice (**B**) and 4T1 tumor-bearing mice treated with vehicle or FEXO (**C**) were analyzed by flow cytometry (n=5-6, t-test). (**D**) Quantification of lung metastatic nodules in vehicle- or FEXO-treated mice with surgical removal of B16-GM primary tumors at early stage (n=5, t-test). Mean ± SEM, **P*<0.05, ***P*<0.01.

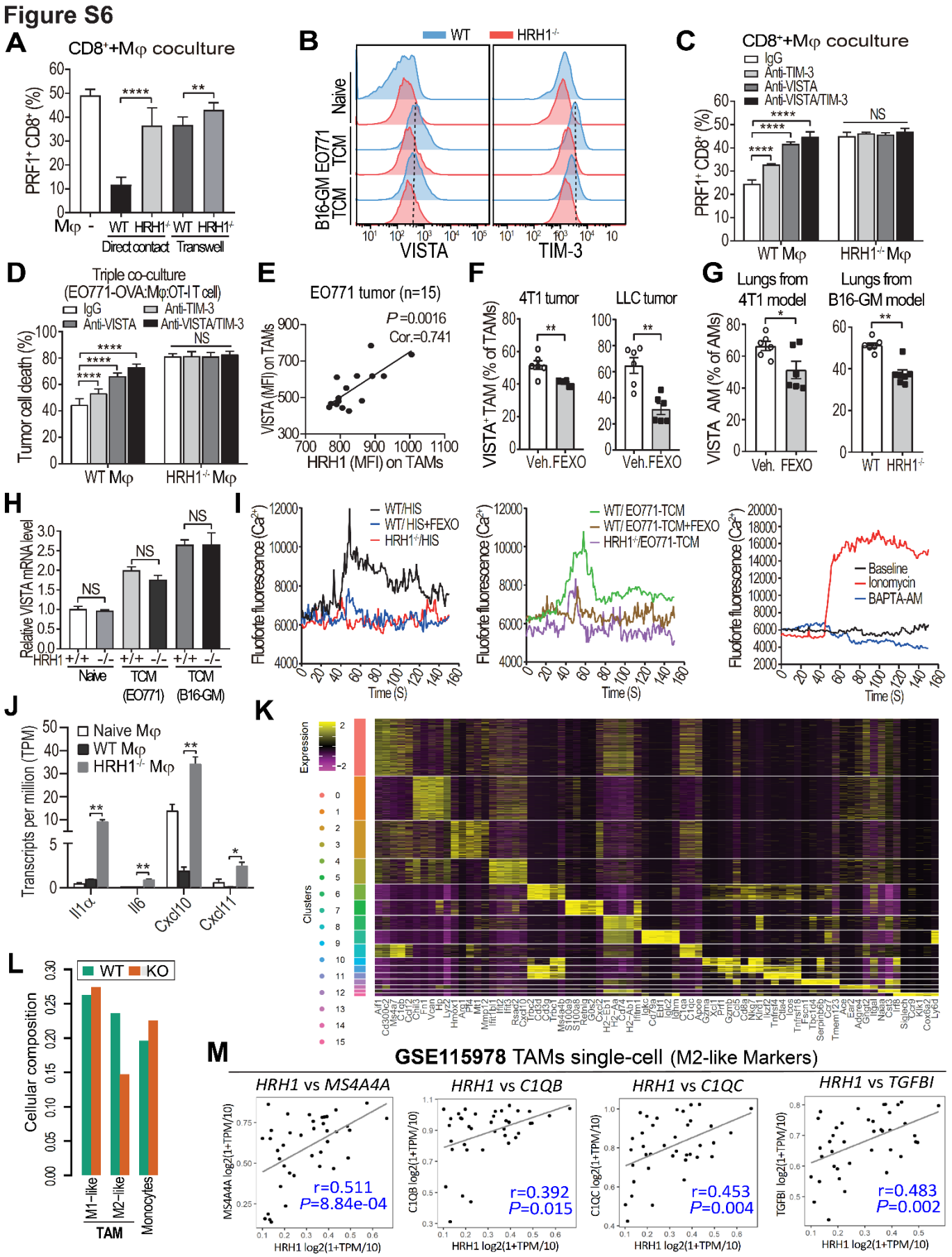

Figure S6. HRH1 activation up-regulates membrane VISTA on macrophages, related to Figures 4 and 5.

(**A**) Percentages of splenic PRF1^{+} CD8^{+} T cells co-cultured with EO771 TCM-treated WT or HRH1$^{-/-}$ BMDMs in a direct-contact or separately in transwells (n=6, t-test). (**B**) Representative flow cytometry plots of VISTA and TIM-3 expression on naïve or TCM-treated WT or HRH1$^{-/-}$ BMDMs. (**C**) Percentages of splenic PRF1^{+} CD8^{+} T cells co-cultured with TCM-treated WT or HRH1$^{-/-}$ BMDMs pretreated with anti-TIM-3 (10 μg/ml), anti-VISTA (10 μg/ml)

antibodies, or combination of them (n=3-4, one-way ANOVA). (**D**) Evaluation of OT1-mediated killing of EO771-OVA cells in the presence of BMDM pretreated with IgG, anti-TIM-3 (10 μg/ml), anti-VISTA (10 μg/ml) antibodies, or combination of them (n=6, one-way ANOVA). (**E**) Pearson correlation between HRH1 and VISTA expression (MFI) on TAMs from EO771 tumors (n=15). (**F**) Flow cytometry analysis of $VISTA^+$ TAMs in 4T1 or LLC tumor tissues from mice treated with vehicle *versus* FEXO (n=6, t-test). (**G**) Flow cytometry analysis of $VISTA^+$ AMs in lung tissues from mice treated with vehicle *versus* FEXO (4T1 tumors), or WT *versus* $HRH1^{-/-}$ mice (B16-GM tumors) (n=6, t-test). (**H**) Relative mRNA level of VISTA in naïve or TCM-treated WT and $HRH1^{-/-}$ BMDMs (n=6, t-test). (**I**) Mobilization of intracellular calcium determined by Fluo-Forte calcium assay. The intracellular calcium concentration was indicated by Fluo-Forte fluorescence. HIS (histamine), 1 μM; FEXO, 10 μM; ionomycin-Ca^{2+}, 1 μg/ml; BAPTA-AM, 10 μM. (**J**) The expression of indicated genes in naïve, TCM-treated WT and $HRH1^{-/-}$ BMDM. (**K**) Gene expression heatmap showing the top 5 highly expressed marker genes between clusters. Gene expression scale is beneath the heatmap, together with the color annotations for cluster identity. (**L**) Bar chart showing different cellular composition of monocytes/macrophage subsets between HRH1-knockout (KO) and WT mice groups. (**M**) Scatter-plot results from the Pearson's correlation analysis of *HRH1* and indicated M2-like macrophage markers at single-cell level in TAMs of human melanomas (GSE115978). Mean ± SEM, all *in vitro* experiments were performed at least three times. **P*<0.05, ***P*<0.01, *****P*<0.0001, NS: not significant.

Figure S7

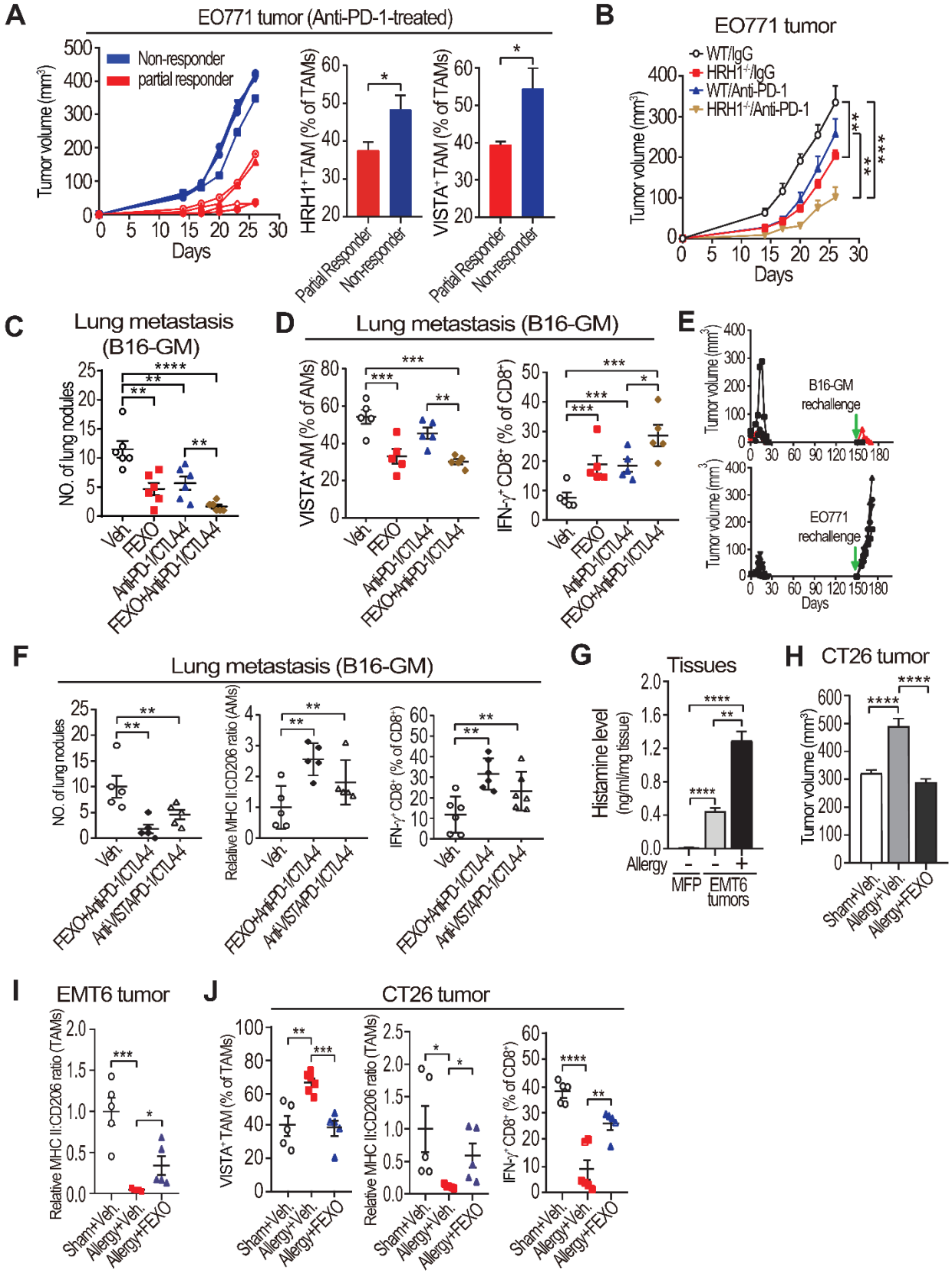

Figure S7. H1-antihistamines synergize with ICB therapy and rescue cancer cell- and allergy-induced immune suppression, related to Figures 6 and 7.

(**A**) EO771 tumor growth and HRH1^{+}/VISTA^{+} TAMs from partial responders *versus* non-responders (n=4, t-test). (**B**) EO771 tumor growth in WT and HRH1$^{-/-}$ mice treated with IgG or anti-PD-1 antibody (n=7-13 mice/group, two-way ANOVA). (**C**) Lung metastasis of B16-GM tumor-bearing WT mice treated with ICB alone, FEXO alone, or ICB+FEXO (n=6, one-way ANOVA). (**D**) Flow cytometry analysis of VISTA^{+} TAMs and IFN-γ^{+} CD8^{+} T cells in lung tissues from B16-GM-bearing mice treated with indicated regimens (n=5, one-way ANOVA). (**E**) Tumor growth in mice

that had complete B16-GM tumor remission in FEXO+ICB group followed by B16-GM or EO771 cell re-challenging (4 mice/each group). (**F**) Quantification of metastatic lung nodules, relative MHC II:CD206 MFI ratios of AMs, and IFN-γ^+ $CD8^+$ T cells in lung tissues from mice-bearing B16-GM tumor treated with indicated regimens (n=5-6, one-way ANOVA). (**G**) Histamine levels detected by ELISA in normal mammary tissue and EMT6 tumors with or without induced allergic reaction (n=3, one-way ANOVA). (**H**) CT26 tumor growth in allergic or sham control mice, followed by vehicle or FEXO treatment (n=7-8 mice/group, two-way ANOVA for tumor volume comparison). (**I**) Analysis of relative MHC II:CD206 MFI ratio (TAMs) in EMT6 tumors from sham control mice, allergic mice, and allergic mice treated with FEXO (n=5, t-test). (**J**) Analysis of $VISTA^+$ TAMs, relative MHC II:CD206 MFI ratio of TAMs and IFN-γ^+ $CD8^+$ T cells in CT26 tumors from sham control mice or allergic mice treated with vehicle or FEXO (n=5-6, t-test). Mean ± SEM, **P*<0.05, ***P*<0.01, ****P*<0.001, *****P*<0.0001.

Table S3. Allergy information of cancer patients, related to Figure 7.

Patient Cancer type	Allergy status reported	No allergy status reported	Sum
Melanoma (2016-2017)	150	728	878
Breast Cancer (2016-2018)	88	254	342
Lung Cancer (2016-2018)	318	1619	1937
Colon Cancer (2016-2018)	100	287	387

Table S4. Responses of anti-PD-1-treated lung cancer patients (n=48) and distributions of their age, sex, and tumor stage with indicated plasma histamine levels, related to Figure 7.

		Treatment response				Age			Gender		TNM stage	
		CR	PR	SD	PD	>70 Ys	50-70 Ys	<50 Ys	Male	Female	III	IV
Histamine	Low (<0.3 ng/ml)	1	9	6	2	5	10	3	16	2	4	14
	Medium (0.3-0.6 ng/ml)	0	7	6	6	3	14	2	15	4	6	13
	High (≥ 0.6 ng/ml)	0	2	3	6	2	7	2	9	2	3	8

Table S5. Responses of anti-PD-1-treated colon cancer patients (n=12) and distributions of their age, sex, and tumor stage with indicated plasma histamine levels, related to Figure 7.

		Treatment response			Age			Gender		TNM stage	
		PR	SD	PD	>70 Ys	50-70 Ys	<50 Ys	Male	Female	III	IV
Histamine	Low (<0.3 ng/ml)	0	0	0	0	0	0	0	0	0	0
	Medium (0.3-0.6 ng/ml)	2	1	1	2	0	2	4	0	1	3
	High (≥ 0.6 ng/ml)	2	2	4	3	3	2	6	2	1	7

Table S6. Responses of anti-PD-1-treated breast cancer patients (n=10) and distributions of their age, sex, and tumor stage with indicated plasma histamine levels, related to Figure 7.

		Treatment response			Age			Gender		TNM stage	
		PR	SD	PD	>70 Ys	50-70 Ys	<50 Ys	Male	Female	III	IV
Histamine	Low (<0.3 ng/ml)	0	0	0	0	0	0	0	0	0	0
	Medium (0.3-0.6 ng/ml)	1	2	1	0	3	1	0	4	0	4
	High (≥ 0.6 ng/ml)	0	2	4	1	4	1	0	6	1	5